AERODYNAMIC DESIGN METHODS

by

Antony Jameson
Princeton University, Princeton, New Jersey, USA

in

Solution Techniques for Large-Scale CFD Problems

Edited by W.G. Habashi
John Wiley & Sons, Ltd.
England

1995

Aerodynamic Design Methods

Antony Jameson
Department of Mechanical and Aerospace Engineering
Princeton University
Princeton, New Jersey, 08544 U.S.A.

1 Introduction

Computational fluid dynamics (CFD) has reached a certain level of maturity in the development of robust algorithms which can accurately treat compressible flows containing shock waves and contact discontinuities. CFD is still not being exploited as effectively as one would like in the design process, however, because of the long set up times and high costs, both human and computational, of complex flow simulations. The principal requirements of effective CFD methods for engineering design are

1. assured accuracy
2. acceptable computational cost
3. fast turn around

Improvements are still needed in all three areas. Effective use of CFD for design is presently limited by the lack of good interfaces to CAD systems, which prevent full automation of the mesh generation process. This bottleneck needs to be eliminated and the CFD system should be fully integrated in a numerical design environment.

The fidelity of mathematical modelling of high Reynolds number flows continues to be limited by computational costs , thus, accurate and cost-effective simulation of viscous flow at high Reynolds numbers associated with full scale flight remains a challenge.

In addition to more accurate and cost-effective flow prediction methods, better optimization methods are also needed, so that not only can designs be rapidly evaluated, but directions of improvement can be identified which enable the rapid evaluation of a satisfactory design. Possession of techniques which result in a faster design cycle gives a crucial advantage in a competitive environment.

2 The Design Problem as a Control Problem

Aerodynamic design has traditionally been carried out on a cut and try basis, with the aerodynamic expertise of the designer guiding the selection of each shape modification. Although considerable gains in aerodynamic performance have been achieved by this approach, continued improvement will most probably be much more difficult to attain. The subtlety and complexity of fluid flow is such that it is unlikely that repeated trials in an interactive analysis and design procedure can lead to a truly optimum design. Automatic design techniques are therefore needed in order to fully realize the potential improvements in aerodynamic efficiency.

Numerical optimization methods have been applied successfully to some simplified cases, such as two-dimensional airfoils in viscous flows [12] and wings in inviscid flows. However, this approach requires the computation of a large number of flow solutions before an optimum point can be located in the design space.

An alternative approach is to cast the design problem as a search for the shape that will generate the desired pressure distribution. This inverse approach recognizes that the designer usually has an idea of the the kind of pressure distribution that will lead to the desired performance. Thus, it is useful to consider the inverse problem of calculating the shape that will lead to a given pressure distribution. The method has the advantage that, only one flow solution is required to obtain the desired design. Unfortunately, a physically realizable shape may not necessarily exist, unless the pressure distribution satisfies certain constraints. Thus the problem must be very carefully formulated.

A particularly attractive way to circumvent the difficulty that the objective may be unattainable is to regard the design problem as a control problem in which the control is the shape of the boundary. A variety of alternative formulations of the design problem can then be treated systematically within the framework of the mathematical theory for control of systems governed by partial differential equations [9]. This approach to optimal aerodynamic design was introduced by Jameson [4, 5], who examined the design problem for compressible flow with shock waves, and devised adjoint equations to determine the gradient for both potential flow and also flows governed by the Euler equations. More recently Ta'asan, Kuruvila, and Salas, implemented a one shot approach in which the constraint represented by the flow equations is only required to be satisfied by the final converged solution [15]. Pironneau has studied the use of control theory for optimum shape design of systems governed by elliptic equations [10], while adjoint methods have also been used by Baysal and Eleshaky [1].

Suppose that the control is defined by a function $\mathcal{F}(\xi)$ of some independent variable ξ or in the discrete case a vector with componets $\mathcal{F}_i$. Also suppose that the desired objective is measured by a cost function I. This may, for example, measure the deviation from a desired surface pressure distribution, but it can also represent other measures of performance such as lift and drag. Thus the design problem is recast into a numerical optimization procedure. This has the advantage that if the objective, say, of a target pressure distribution, is unattainable, it is still possible to find a minimum of the cost function. Now a variation $\delta\mathcal{F}$ in the control produces a variation δI in the cost. Following control theory, δI can be expressed to first order as an inner product

$$\delta I = (\mathcal{G}, \delta\mathcal{F}),$$

where the gradient $\mathcal{G}$ is independent of the particular variation $\delta\mathcal{F}$, and can be determined by solving an adjoint equation. For a discrete system of equations

$$(\mathcal{G}, \delta\mathcal{F}) \equiv \sum \mathcal{G}_i \delta\mathcal{F}_i$$

and for an infinitely dimensional system

$$(\mathcal{G}, \delta\mathcal{F}) \equiv \int \mathcal{G}(\xi)\, \delta\mathcal{F}\, d\xi.$$

In either case, if one makes a shape change

$$\delta\mathcal{F} = -\lambda\mathcal{G}, \tag{1}$$

where λ is sufficiently small and positive, then

$$\delta I = -\lambda(\mathcal{G}, \mathcal{G}) < 0$$

assuring a reduction in I.

For flow about an airfoil or wing, the aerodynamic properties which define the cost function are functions of the flow-field variables (w) and the physical location of the boundary, which may be represented by the function $\mathcal{F}$, say. Then

$$I = I(w, \mathcal{F}),$$

and a change in $\mathcal{F}$ results in a change

$$\delta I = \frac{\partial I^T}{\partial w}\delta w + \frac{\partial I^T}{\partial \mathcal{F}}\delta\mathcal{F}, \tag{2}$$

in the cost function. Brute force methods evaluate the gradient by making a small change in each design variable separately, and then recalculating both the grid and flow-field variables. This requires a number of additional flow calculations equal to the number of design variables. Using control theory, the governing equations of the flowfield are introduced as a constraint in such a way that the final expression for the gradient doas not require reevaluation of the flow field. In order to achieve this δw must be eliminated from (2). The governing equation R expresses the dependence of w and $\mathcal{F}$ within the flowfield domain D,

$$R(w, \mathcal{F}) = 0,$$

Thus δw is determined from the equation

$$\delta R = \left[\frac{\partial R}{\partial w}\right]\delta w + \left[\frac{\partial R}{\partial \mathcal{F}}\right]\delta\mathcal{F} = 0. \tag{3}$$

Next, introducing a Lagrange Multiplier ψ, we have

$$\begin{aligned}\delta I &= \frac{\partial I^T}{\partial w}\delta w + \frac{\partial I^T}{\partial \mathcal{F}}\delta \mathcal{F} - \psi^T\left(\left[\frac{\partial R}{\partial w}\right]\delta w + \left[\frac{\partial R}{\partial \mathcal{F}}\right]\delta \mathcal{F}\right) \\ &= \left\{\frac{\partial I^T}{\partial w} - \psi^T\left[\frac{\partial R}{\partial w}\right]\right\}\delta w + \left\{\frac{\partial I^T}{\partial \mathcal{F}} - \psi^T\left[\frac{\partial R}{\partial \mathcal{F}}\right]\right\}\delta \mathcal{F}\end{aligned}$$

Choosing ψ to satisfy the adjoint equation

$$\left[\frac{\partial R}{\partial w}\right]^T \psi = \frac{\partial I}{\partial w} \tag{4}$$

the first term is eliminated, and we find that

$$\delta I = \mathcal{G}\delta \mathcal{F} \tag{5}$$

where

$$G = \frac{\partial I^T}{\partial \mathcal{F}} - \psi^T\left[\frac{\partial R}{\partial \mathcal{F}}\right].$$

The advantage is that (5) is independent of δw, with the result that the gradient of I with respect to an arbitrary number of design variables can be determined without the need for additional flow-field evaluations. The main cost is in solving the adjoint equation (4). In general, the adjoint problem is about as complex as a flow solution. If the number of design variables is large, the cost differential between one adjoint solution and the large number of flowfield evaluations required to determine the gradient by brute force becomes compelling. Instead of introducing a Lagrange multiplier, ψ, one can solve (3) for δw as

$$\delta w = -\left[\frac{\partial R}{\partial w}\right]^{-1}\left[\frac{\partial R}{\partial \mathcal{F}}\right]\delta \mathcal{F},$$

and insert the result in (2). This is the implicit gradient approach, which is essentially equivalent to the control theory approach, as has been pointed out by Shubin and Frank [13, 14]. In any event there is and advantage in determining the gradient $\mathcal{G}$ by the solution of the adjoint equation.

After making such a modification, the gradient can be recalculated and the process repeated to follow a path of steepest descent (1) until a minimum is reached. In order to avoid violating constraints, such as a minimum acceptable wing thickness, the gradient may be projected into the allowable subspace within which the constraints are satisfied. In this way one can devise procedures which must necessarily converge at least to a local minimum, and which can be accelerated by the use of more sophisticated descent methods such as conjugate gradient or quasi-Newton algorithms. There is the possibility of more than one local minimum, but in any case the method will lead to an improvement over the original design. Furthermore, unlike the traditional inverse algorithms, any measure of performance can be used as the cost function.

In order to illustrate the application of control theory to aerodynamic design problems the next section presents the method for three-dimensional wing design using the inviscid Euler equations as the mathematical model for compressible flow.

3 Three Dimensional Design Using the Euler Equations

It proves convenient to denote the Cartesian coordinates and velocity components by x_1, x_2, x_3 and u_1, u_2, u_3, and to use the convention that summation over $i = 1$ to 3 is implied by a repeated index i. The three-dimensional Euler equations may be written as

$$\frac{\partial w}{\partial t} + \frac{\partial f_i}{\partial x_i} = 0 \quad \text{in } D, \tag{6}$$

where

$$w = \begin{Bmatrix} \rho \\ \rho u_1 \\ \rho u_2 \\ \rho u_3 \\ \rho E \end{Bmatrix}, \quad f_i = \begin{Bmatrix} \rho u_i \\ \rho u_i u_1 + p\delta_{i1} \\ \rho u_i u_2 + p\delta_{i2} \\ \rho u_i u_3 + p\delta_{i3} \\ \rho u_i H \end{Bmatrix} \tag{7}$$

and δ_{ij} is the Kronecker delta function. Also,

$$p = (\gamma - 1)\rho\left\{E - \frac{1}{2}\left(u_i^2\right)\right\}, \tag{8}$$

and

$$\rho H = \rho E + p \tag{9}$$

where γ is the ratio of the specific heats. Consider a transformation to coordinates ξ_1, ξ_2, ξ_3 where

$$K_{ij} = \left[\frac{\partial x_i}{\partial \xi_j}\right], \quad J = \det(K), \quad K_{ij}^{-1} = \left[\frac{\partial \xi_i}{\partial x_j}\right].$$

Introduce contravariant velocity components as

$$\begin{Bmatrix} U_1 \\ U_2 \\ U_3 \end{Bmatrix} = K^{-1} \begin{Bmatrix} u_1 \\ u_2 \\ u_3 \end{Bmatrix}$$

The Euler equations can now be written as

$$\frac{\partial W}{\partial t} + \frac{\partial F_i}{\partial \xi_i} = 0 \quad \text{in } D, \tag{10}$$

with

$$W = J\begin{Bmatrix} \rho \\ \rho u_1 \\ \rho u_2 \\ \rho u_3 \\ \rho E \end{Bmatrix}, \; F_i = J\begin{Bmatrix} \rho U_i \\ \rho U_i u_1 + \frac{\partial \xi_i}{\partial x_1} p \\ \rho U_i u_2 + \frac{\partial \xi_i}{\partial x_2} p \\ \rho U_i u_3 + \frac{\partial \xi_i}{\partial x_3} p \\ \rho U_i H \end{Bmatrix}. \tag{11}$$

Assume now that the new computational coordinate system conforms to the wing in such a way that the wing surface B_W is represented by $\xi_2 = 0$. Then the flow is determined as the steady state solution of equation (10) subject to the flow tangency condition

$$U_2 = 0 \quad \text{on } B_W. \tag{12}$$

At the far field boundary B_F, conditions are specified for incoming waves while outgoing waves are determined by the solution.

Suppose now that it is desired to control the surface pressure by varying the wing shape. It is convenient to retain a fixed computational domain. Variations in the shape then result in corresponding variations in the mapping derivatives defined by H. Introduce the cost function

$$I = \frac{1}{2}\iint_{B_W} (p - p_d)^2 \, d\xi_1 d\xi_3,$$

where p_d is the desired pressure. The design problem is now treated as a control problem where the control function is the wing shape, which is to be chosen to minimize I subject to the constraints defined by the flow equations (10–11). A variation in the shape will cause a variation δp in the pressure and consequently the a variation in the cost function

$$\delta I = \iint_{B_W} (p - p_d)\, \delta p \; d\xi_1 d\xi_3. \tag{13}$$

Since p depends on w through the equation of state (8–9), the variation δp can be determined from the variation δw. Define the Jacobian matrices

$$A_i = \frac{\partial f_i}{\partial w}, \quad C_i = J K_{ij}^{-1} A_j. \tag{14}$$

Then the equation for δw in the steady state becomes

$$\frac{\partial}{\partial \xi_i}\left(\delta F_i\right) = 0, \tag{15}$$

where

$$\delta F_i = C_i \delta w + \delta\left(J\frac{\partial \xi_i}{\partial x_j}\right) f_j.$$

Now, multiplying by a vector co-state variable ψ and integrating over the domain

$$\int_{D_j} \psi^T \left(\frac{\partial \delta F_i}{\partial \xi_i}\right) d\xi_j = 0,$$

and if ψ is differentiable this may be integrated by parts to give

$$\int_{D_j} \left(\frac{\partial \psi^T}{\partial \xi_i}\delta F_i\right) d\xi_j = \int_B \left(n_i \psi^T \delta F_i\right) d\xi_B,$$

where n_i are components of a unit vector normal to the boundary. Thus the variation in the cost function may now be written

$$\delta I = \iint_{B_W} \left(p - p_d\right) \delta p \;\; d\xi_1 d\xi_3 - \int_{D_j} \left(\frac{\partial \psi^T}{\partial \xi_i}\delta F_i\right) d\xi_j + \int_B \left(n_i \psi^T \delta F_i\right) d\xi_B. \tag{16}$$

On the wing surface B_W, $n_1 = n_3 = 0$ and it follows from equation (12) that

$$\delta F_2 = J \begin{Bmatrix} 0 \\ \frac{\partial \xi_2}{\partial x_1}\delta p \\ \frac{\partial \xi_2}{\partial x_2}\delta p \\ \frac{\partial \xi_2}{\partial x_3}\delta p \\ 0 \end{Bmatrix} + p \begin{Bmatrix} 0 \\ \delta\left(J\frac{\partial \xi_2}{\partial x_1}\right) \\ \delta\left(J\frac{\partial \xi_2}{\partial x_2}\right) \\ \delta\left(J\frac{\partial \xi_2}{\partial x_3}\right) \\ 0 \end{Bmatrix}. \tag{17}$$

Suppose now that ψ is the steady state solution of the adjoint equation

$$\frac{\partial \psi}{\partial t} - C_i^T \frac{\partial \psi}{\partial \xi_i} = 0 \quad \text{in } D. \tag{18}$$

At the outer boundary incoming characteristics for ψ correspond to outgoing characteristics for δw. Consequently, one can choose boundary conditions for ψ such that

$$n_i \psi^T C_i \delta w = 0.$$

Then if the coordinate transformation is such that $\delta\left(JK^{-1}\right)$ is negligible in the far field, the only remaining boundary term is

$$-\iint_{B_W} \psi^T \delta F_2 \; d\xi_1 d\xi_3.$$

Thus by letting ψ satisfy the boundary condition,

$$J\left(\psi_2 \frac{\partial \xi_2}{\partial x_1} + \psi_3 \frac{\partial \xi_2}{\partial x_2} + \psi_4 \frac{\partial \xi_2}{\partial x_3}\right) = \left(p - p_d\right) \;\; \text{on } B_W, \tag{19}$$

we find finally that

$$\begin{aligned} \delta I = & \int_D \frac{\partial \psi^T}{\partial \xi_i}\delta\left(J\frac{\partial \xi_i}{\partial x_j}\right) f_j d\xi_D \\ & - \iint_{B_W} \left\{\psi_2 \frac{\partial \xi_2}{\partial x_1} + \psi_3 \frac{\partial \xi_2}{\partial x_2} + \psi_4 \frac{\partial \xi_2}{\partial x_3}\right\} p \, d\xi_1 d\xi_3. \end{aligned} \tag{20}$$

1a: x, y-Plane.

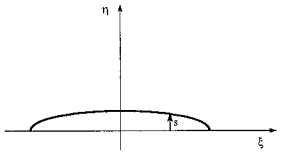

1b: ξ, η-Plane.

Figure 1: Sheared Parabolic Mapping.

A convenient way to treat a wing is to introduce sheared parabolic coordinates as shown in figure 1 through the transformation

$$\begin{aligned} x &= x_0(\zeta) + \frac{1}{2}a(\zeta)\left\{\xi^2 - (\eta + \mathcal{S}(\xi,\zeta))^2\right\} \\ y &= y_0(\zeta) + a(\zeta)\,\xi\,(\eta + \mathcal{S}(\xi,\zeta)) \\ z &= \zeta. \end{aligned}$$

Here $x = x_1$, $y = x_2$, $z = x_3$ are the Cartesian coordinates, and ξ and $\eta + \mathcal{S}$ correspond to parabolic coordinates generated by the mapping

$$x + iy = x_0 + iy_0 + \frac{1}{2}a(\zeta)\{\xi + i(\eta + \mathcal{S})\}^2$$

at a fixed span station ζ. $x_0(\zeta)$ and $y_0(\zeta)$ are the coordinates of a singular line which is swept to lie just inside the leading edge of a swept wing, while $a(\zeta)$ is a scale factor to allow for spanwise chord variations. The surface $\eta = 0$ is a shallow bump corresponding to the wing surface, with a height $\mathcal{S}(\xi,\zeta)$ determined by the equation

$$\xi + i\mathcal{S} = \sqrt{2\,(x_{B_W} + iy_{B_W})},$$

where $x_{B_W}(z)$ and $y_{B_W}(z)$ are coordinates of points lying on the wing surface. We now treat $\mathcal{S}(\xi,\zeta)$ as the control.

In this case the transformation matrix $\frac{\partial x_i}{\partial \xi_j}$ becomes

$$\begin{aligned} K &= \begin{bmatrix} a\left(\xi - (\eta+\mathcal{S})\mathcal{S}_\xi\right) & -a(\eta+\mathcal{S}) & \mathcal{A} - a(\eta+\mathcal{S})\mathcal{S}_\zeta \\ a\left(\eta + \mathcal{S} + \xi\mathcal{S}_\xi\right) & a\xi & \mathcal{B} + a\xi\mathcal{S}_\zeta \\ 0 & 0 & 1 \end{bmatrix} \\ &= \begin{bmatrix} x_\xi & x_\eta & \mathcal{A} + x_\eta\mathcal{S}_\zeta \\ y_\xi & y_\eta & \mathcal{B} + y_\eta\mathcal{S}_\zeta \\ 0 & 0 & 1 \end{bmatrix}, \end{aligned}$$

where

$$\mathcal{A} = a_\zeta\frac{x - x_0}{a} + x_{0_\zeta}, \quad \mathcal{B} = a_\zeta\frac{y - y_0}{a} + y_{0_\zeta}.$$

Now,

$$J = x_\xi y_\eta - x_\eta y_\xi = \xi^2 + (\eta + \mathcal{S})^2$$

and

$$JK^{-1} = \begin{bmatrix} y_\eta & -x_\eta & x_\eta\mathcal{B} - y_\eta\mathcal{A} \\ -y_\xi & x_\xi & y_\xi\mathcal{A} - x_\xi\mathcal{B} - J\mathcal{S}_\zeta \\ 0 & 0 & J \end{bmatrix}.$$

Then under a modification $\delta\mathcal{S}$

$$\begin{aligned} \delta x_\xi &= -a\left(\delta\mathcal{S}\mathcal{S}_\xi + (\eta+\mathcal{S})\,\delta\mathcal{S}_\xi\right) \\ \delta x_\eta &= -a\delta\mathcal{S} \\ \delta y_\xi &= a\left(\delta\mathcal{S} + \xi\delta\mathcal{S}_\xi\right) \\ \delta y_\eta &= 0. \end{aligned}$$

Thus

$$\delta J = 2a^2 (\eta + \mathcal{S}) \delta \mathcal{S}$$

and

$$\delta \left(J K^{-1} \right) = \begin{bmatrix} 0 & a\delta\mathcal{S} & -a\mathcal{B}\delta\mathcal{S} \\ -\delta y_\xi & \delta x_\xi & \mathcal{D} \\ 0 & 0 & \delta J \end{bmatrix}.$$

where

$$\mathcal{D} = \delta y_\xi \mathcal{A} - \delta x_\xi \mathcal{B} - a_\zeta \frac{J}{a} \delta\mathcal{S} - \delta J \mathcal{S}_\zeta - J\delta\mathcal{S}_z.$$

Inserting these formulas in equation (20) we find that the volume integral in δI is

$$\begin{aligned} & \iiint \frac{\partial \psi^T}{\partial \xi} \delta\mathcal{S} f_2 \, d\xi \, d\eta \, d\zeta \\ - & \iiint \frac{\partial \psi^T}{\partial \eta} \left\{ -\delta y_\xi f_1 + \delta x_\xi f_2 + \mathcal{D} f_3 \right\} d\xi \, d\eta \, d\zeta \\ + & \iiint \frac{\partial \psi^T}{\partial \zeta} \delta J f_3 \, d\xi \, d\eta \, d\zeta, \end{aligned}$$

where $\mathcal{S}$ and $\delta\mathcal{S}$ are independent of η. Therefore, integrating over η, the variation in the cost function can be reduced to a surface integral of the form

$$\delta I = \iint_{B_W} \left(P(\xi,\zeta) \delta\mathcal{S} - Q(\xi,\zeta) \delta\mathcal{S}_\xi - R(\xi,\zeta) \delta\mathcal{S}_\zeta \right) d\xi \, d\zeta$$

Here

$$\begin{aligned} P &= a (\psi_2 + \mathcal{S}_\xi \psi_3 + \mathcal{C}\psi_4) p \\ &- \int \frac{\partial \psi^T}{\partial \xi} \left\{ \xi f_1 + (\eta + \mathcal{S}) f_2 + (\xi\mathcal{A} + (\eta + \mathcal{S}) \mathcal{B}) f_3 \right\} d\eta \\ &- \int \frac{\partial \psi^T}{\partial \eta} (f_1 + \mathcal{S}_\xi f_2 + \mathcal{C} f_3) \, d\eta \\ &- \int \frac{\partial \psi^T}{\partial \zeta} J d\eta \end{aligned}$$

$$\begin{aligned} Q &= a (\xi\psi_2 + (\eta + \mathcal{S}) \psi_3) p \\ &+ \int \frac{\partial \psi^T}{\partial \eta} \left\{ \xi f_1 + (\eta + \mathcal{S}) f_2 + (\xi\mathcal{A} + (\eta + \mathcal{S}) \mathcal{B}) f_3 \right\} d\eta \end{aligned}$$

$$\begin{aligned} R &= J\psi_4 p \\ &+ \int \frac{\partial f_3}{\partial \eta} J\psi_4 d\eta, \end{aligned}$$

where

$$\mathcal{C} = 2a (\eta + \mathcal{S}) \mathcal{S}_\zeta - \mathcal{A} - \mathcal{B}\mathcal{S}_\xi + \frac{J}{a}.$$

Also the shape change will be confined to a boundary region of the $\xi - \zeta$ plane, so we can integrate by parts to obtain

$$\delta I = \iint_{B_W} \left(P + \frac{\partial Q}{\partial \xi} + \frac{\partial R}{\partial \zeta} \right) \delta\mathcal{S} \; d\xi \, d\zeta.$$

Thus to reduce I we can choose

$$\delta\mathcal{S} = -\lambda \left(P + \frac{\partial Q}{\partial \xi} + \frac{\partial R}{\partial \zeta} \right),$$

where λ is sufficiently small and non-negative.

In order to impose a thickness constraint we can define a baseline surface $\mathcal{S}_0(\xi,\zeta)$ below which $\mathcal{S}(\xi,\zeta)$ is not allowed to fall. Now if we take $\lambda = \lambda(\xi,\zeta)$ as a non-negative function such that

$$\mathcal{S}(\xi,\zeta) + \delta\mathcal{S}(\xi,\zeta) \geq \mathcal{S}_0(\xi,\zeta).$$

Then the constraint is satisfied, while

$$\delta I = -\iint_{B_W} \lambda \left(P + \frac{\partial Q}{\partial \xi} + \frac{\partial R}{\partial \zeta} \right)^2 d\xi \, d\zeta \leq 0.$$

4 Implementation for swept wings

Since three dimensional calculations require substantial computational resources, it is extremely important for the practical implementation of the method to use fast solution algorithms for the flow and the adjoint equations. In this case the author's FLO87 computer program has been used as the basis of the design method. FLO87 solves the three dimensional Euler equations with a cell-centered finite volume scheme, and uses residual averaging and multigrid acceleration to obtain very rapid steady state solutions, usually in 25 to 50 multigrid cycles [2, 3]. Upwind biasing is used to produce nonoscillatory solutions, and assure the clean capture of shock waves. This is introduced through the addition of carefully controlled numerical diffusion terms, with a magnitude of order Δx^3 in smooth parts of the flow. The adjoint equations are treated in the same way as the flow equations. The fluxes are first estimated by central differences, and then modified by downwind biasing through numerical diffusive terms which are supplied by the same subroutines that were used for the flow equations.

The method has been tested for the optimization of a swept wing. The wing planform was fixed while the sections were free to be changed arbitrarily by the design method, with a restriction on the minimum thickness. The wing has a unit-semi-span, with 38 degrees leading edge sweep. It has a modified trapezoidal planform, with straight taper from a root chord of 0.38, and a curved trailing edge in the inboard region blending into straight taper outboard of the 30 percent span station to a tip chord of 0.10, with an aspect ration of 9.0. The initial wing sections were based on a section specifically designed by the author's two dimensional design method [4] to give shock free flow at Mach 0.78 with a lift coefficient of 0.6. The pressure distribution is displayed in figure 2. This section, which has a thickness to chord ration of 9.5 percent, was used at the tip. Similar sections with an increased thickness were used inboard. The variation of thickness was non-linear with a more rapid increase near the root, where the thickness to chord ratio of the basic section was multiplied by a factor of 1.47. The inboard sections were rotated upwards to give the initial wing 3. degrees twist from root to tip. The two dimensional pressure distribution of the basic wing section at its design point was introduced as a target pressure distribution uniformly across the span. This target is presumably not realizable, but serves to favor the establishment of relatively benign pressure distribution. The total inviscid drag coefficient, due to the combination of vortex and shock wave drag, was also included in the cost function. Calculations were performed with the lift coefficient forced to approach a fixed value by adjusting the angle of attack every fifth iteration of the flow solution. It was found that the computational costs can be reduced by using only 15 multigrid cycles in each flow solution, and in each adjoint solution. Although this is not enough for full convergence, it proves sufficient to provide a shape modification which leads to an improvement.

Figures 3 and 4 show the result of a calculation at Mach number of 0.85, with the lift coefficient forced to approach a value of 0.5. This calculation was performed on a mesh with 192 intervals in the ξ direction wrapping around the wing, 32 intervals in the normal η direction and 48 intervals in the spanwise ζ direction, giving a total of 294912 cells. The wing was specified by 33 sections, each with 128 points, giving a total of 4224 design variables. The plots show the initial wing geometry and pressure distribution, and the modified geometry and pressure distribution after 10 design cycles. The total inviscid drag coefficient was reduced from 0.0209 to 0.0119. The initial design exhibits a very strong shock wave in the inboard region. It can be seen that this is completely eliminated, leaving a very weak shock wave in the outboard region. The drag reduction is mainly accomplished in the first four design cycles but the pressure distribution continues to be adjusted to become more like the target pressure distribution. To verify the solution, the final geometry, after 10 design cycles, was analyzed with another method using the computer program FLO67. This program uses a cell-vertex formulation, and has recently been modified to incorporate a local extremum diminishing algorithm with a very low level of numerical diffusion [6]. When run to full convergence it was found that the redesigned wing has a drag coefficient of 0.0096 at Mach 0.85 at a lift coefficient of 0.5, with a corresponding lift to drag ratio of 52. The result for $\alpha = 0.0°$ and $C_L = 0.505$ is illustrated in Figure 5: this seems to be the nearest to a shock free condition. A calculation at Mach 0.500 shows a drag coefficient of 0.0089 for a lift coefficient of 0.5. Since in this case the flow is entirely subsonic, this provides an estimate of the vortex drag for this planform and lift distribution, which is just what one obtains from the standard formula for induced drag, $C_D = {C_L}^2/\epsilon\pi AR$, with an aspect ratio $AR = 9$, and an efficiency factor $\epsilon = 0.97$. Thus the design method has reduced the shock wave drag coefficient to about 0.0007 at a lift coefficient of 0.5.

Figures 6 and 7 show the result of another optimization starting from the same initial geometry, and at the same mach number of 0.850, but with the lift coefficient increased to 0.55. This produces stronger shock waves and is therefore a more severe test of the method. In this case the total inviscid drag coefficient was reduced from 0.0243 to 0.0144. Again the performance of the final design was verified by a calculation with

FLO67, using a high resolution LED algorithm, and when the result was fully converged the drag coefficient was found to be 0.0119. The result is illustrated in figure 8. A subsonic calculation at Mach .500 shows a drag coefficient of 0.0109 for a lift coefficient of 0.55. Thus in this case the shock wave drag coefficient is about 0.0010.

For a representative transport aircraft the parasite drag coefficient of the wing due to skin friction is about 0.0045. Also the fuselage drag coefficient is about 0.0050, the nacelle drag coefficient is about 0.0015, the empennage drag coefficient is about 0.0020, and excrescence drag coefficient is about 0.0010. This would give a total drag coefficient $C_D = 0.0259$ for a lift coefficient of 0.55, corresponding to a lift to drag ratio $L/D = 21.2$. This would be a substantial improvement over the values obtained by currently flying transport aircraft.

5 Conclusion

In the period since this approach to optimal shape design was first proposed by the author [4], the method has been verified by numerical implementation for both potential flow [5, 7, 11]. and flows modeled by the Euler equations. The results suggest that the method can be a very useful tool for the design of new airplanes. Even in the case of three dimensional flows, the computational requirements are so moderate that the calculations can be performed with workstations such as the IBM RISC 6000 series. A design cycle on a 192x32x48 mesh takes about $1\frac{1}{2}$ hours on an IBM model 530 workstation, allowing overnight completion of a design calculation for a swept wing. The formulation presentd here takes advantage of analytic mesh transormations to simplify the calculation of derivatives of the metric terms. In order to treat more complex geometric configurations it may be necessary to generate the mesh for the initial shape by a numerical method. Then the mesh may be deformed by analytic mesh transformations to accomodate the shape changes in the subsequent design iterations. This method, which enables easy evaluation of the derivatives of the metric terms, has already been demonstrated for two dimensional flows modelled by the Euler equations [8].

Acknowledgments

The author is grateful to James Reuther for his assistance in assembling the text and figures with LaTeX. This research has benefited greatly from the generous support of the AFOSR under grant number AFOSR-91-0391, ARPA under grant number N00014-92-J-1976, USRA through RIACS, and IBM. The warm hospitality of the Aeronautics and Astronautics Department of Stanford University, and NASA Ames Research Center, provided a very favorable enviroment for the pursuit of this research while the author was on leave from Princeton University.

References

[1] O. Baysal and M. E. Eleshaky. Aerodynamic design optimization using sensitivity anaysis and computational fluid dynamics. *AIAA paper 91-0471*, 29th Aerospace Sciences Meeting, Reno, Nevada, January 1991.

[2] A. Jameson. Solution of the Euler equations by a multigrid method. *Applied Mathematics and Computations*, 13:327–356, 1983.

[3] A. Jameson. Multigrid algorithms for compressible flow calculations. In W. Hackbusch and U. Trottenberg, editors, *Lecture Notes in Mathematics, Vol. 1228*, pages 166–201. Proceedings of the 2nd European Conference on Multigrid Methods, Cologne, 1985, Springer-Verlag, 1986.

[4] A. Jameson. Aerodynamic design via control theory. *Journal of Scientific Computing*, 3:233–260, 1988.

[5] A. Jameson. Automatic design of transonic airfoils to reduce the shock induced pressure drag. In *Proceedings of the 31st Israel Annual Conference on Aviation and Aeronautics, Tel Aviv*, pages 5–17, February 1990.

[6] A. Jameson. Artificial diffusion, upwind biasing, limiters and their effect on accuracy and multigrid convergence in transonic and hypersonic flows. *AIAA paper 93-3359*, AIAA 11th Computational Fluid Dynamics Conference, Orlando, Florida, July 1993.

[7] A. Jameson. Computational algorithms for aerodynamic analysis and design. *Appl. Num. Math.*, 13:383–422, 1993.

[8] A. Jameson and J. Reuther. Control theory based airfoil design using the euler equations. *AIAA paper 94-4272*, AIAA-NASA-USAF-SSMO Symposium on Multidisciplinary Analysis and Optimization, Panama City, Fl, September 1994 1994.

[9] J.L. Lions. *Optimal Control of Systems Governed by Partial Differential Equations.* Springer-Verlag, New York, 1971. Translated by S.K. Mitter.

[10] O. Pironneau. *Optimal Shape Design for Elliptic Systems.* Springer-Verlag, New York, 1984.

[11] J. Reuther and A. Jameson. Control theory based airfoil design for potential flow and a finite volume discretization. *AIAA paper 94-499*, 32th Aerospace Sciences Meeting and Exibit, Reno, Nevada, January 1994.

[12] J. Reuther, C.P. van Dam, and R. Hicks. Subsonic and transonic low-Reynolds-number airfoils with reduced pitching moments. *Journal of Aircraft*, 29:297–298, 1992.

[13] G. R. Shubin. Obtaining cheap optimization gradients from computaional aerodynamics codes. *Internal paper AMS-TR-164*, Boeing Computer Services, June 1991.

[14] G. R. Shubin and P. D. Frank. A comparison of the implicit gradient approach and the variational approach to aerodynamic design optimization. *internal paper AMS-TR-164*, Boeing Computer Services, April 1991.

[15] S. Ta'asan, G. Kuruvila, and M. D. Salas. Aerodynamic design and optimization in one shot. *AIAA paper 91-005*, 30th Aerospace Sciences Meeting and Exibit, Reno, Nevada, January 1992.

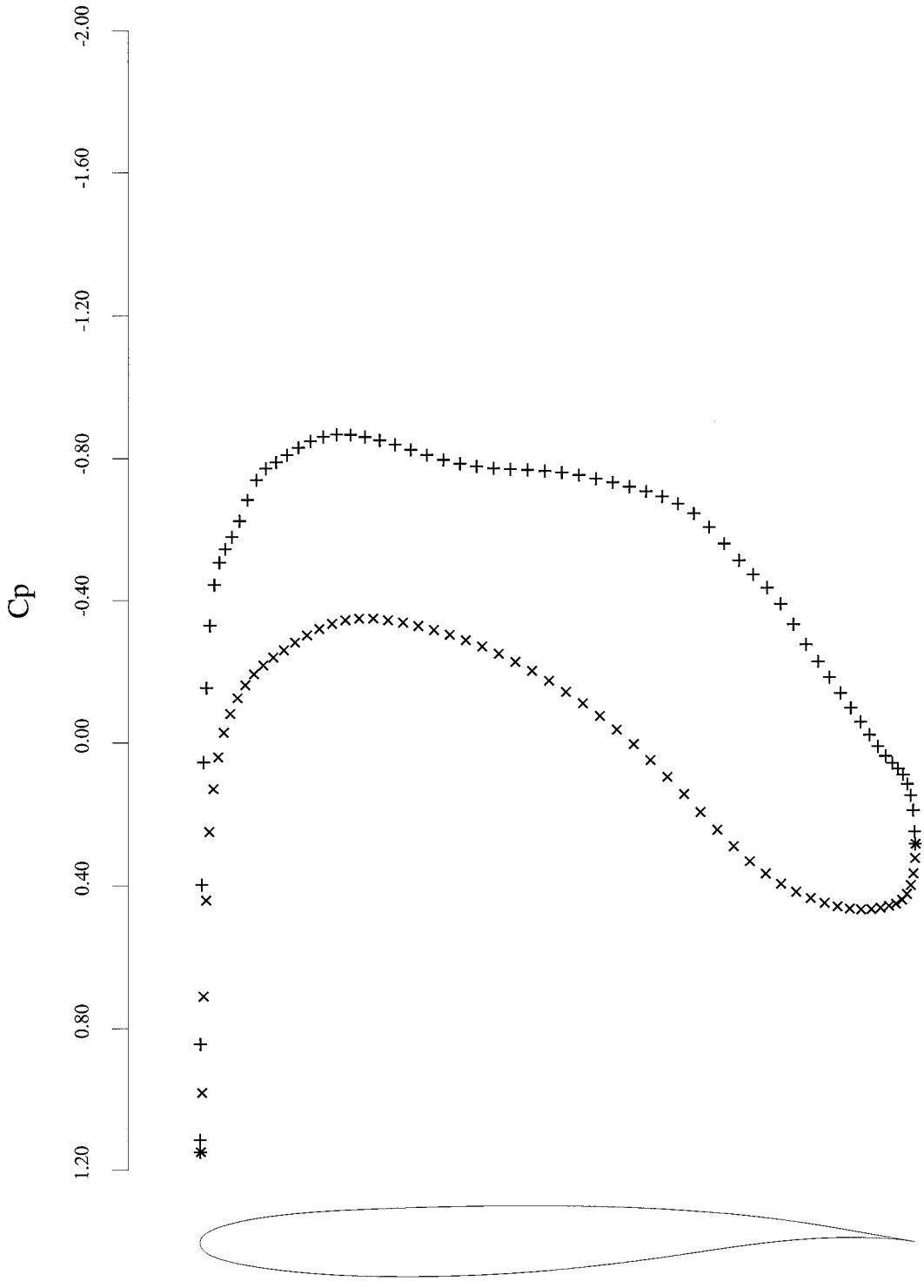

Figure 2: Initial Wing Section and Target Pressure Distribution

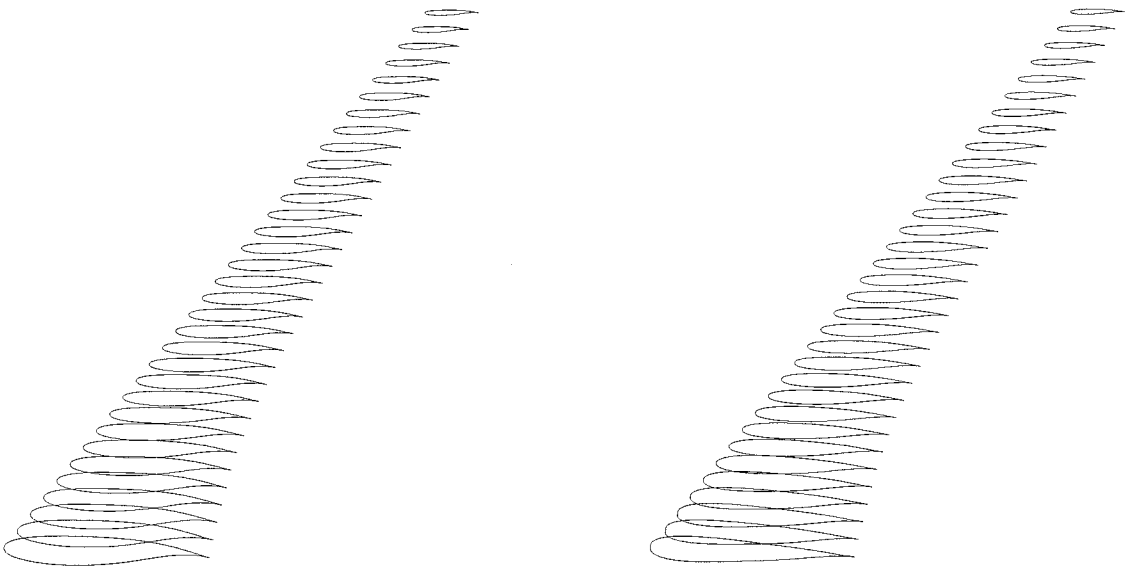

3a: Initial Wing
$C_l = 0.5000$, $C_d = 0.0209$, $\alpha = -1.349°$

3b: 10 Design Iterations
$C_l = 0.5000$, $C_d = 0.0119$, $\alpha = 0.033°$

Figure 3: Lifting Design Case, $M = 0.85$, Fixed Lift Mode.
Drag Reduction

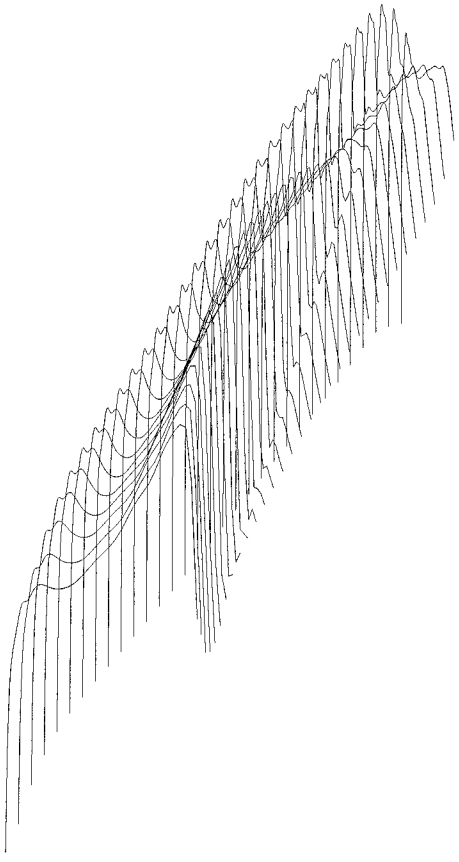

UPPER SURFACE PRESSURE

4a: Initial Wing
Lifting Design Case, $M = 0.85$, Fixed Lift Mode.
$C_L = 0.5000$, $C_D = 0.0209$, $\alpha = -1.349°$
Drag Reduction

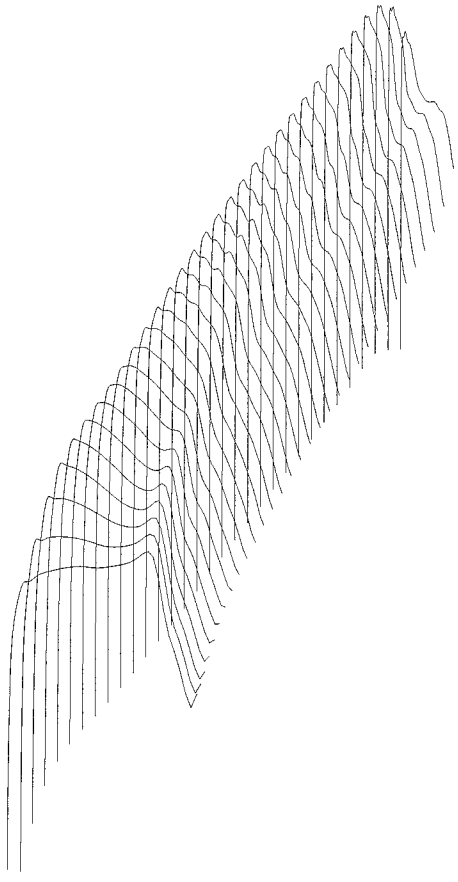

UPPER SURFACE PRESSURE

4b: 10 Design Iterations
Lifting Design Case, $M = 0.85$, Fixed Lift Mode.
$C_L = 0.5000$, $C_D = 0.0119$, $\alpha = 0.033°$
Drag Reduction

Figure 4: Lifting Design Case, $M = 0.85$, Fixed Lift Mode.
Drag Reduction

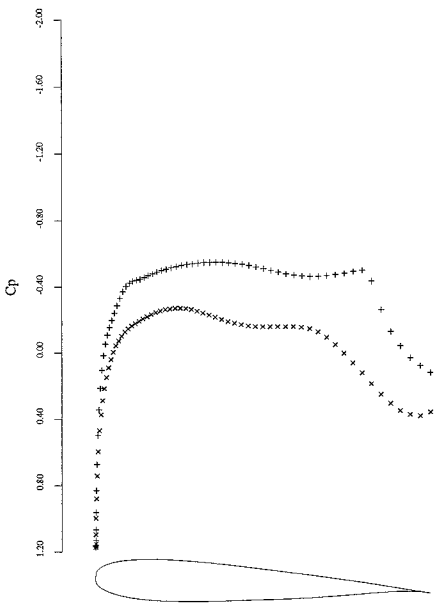

5a: span station $z = 0.00$

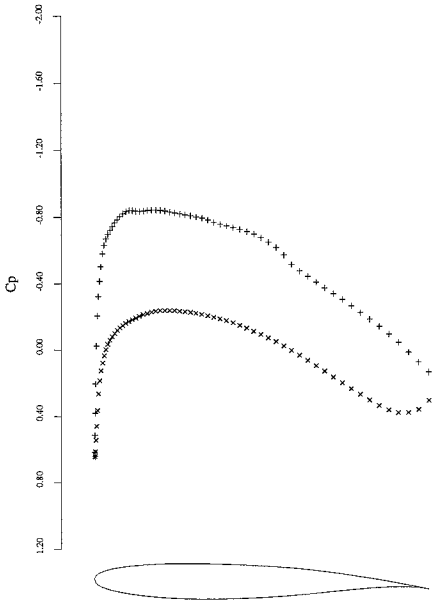

5b: span station $z = 0.312$

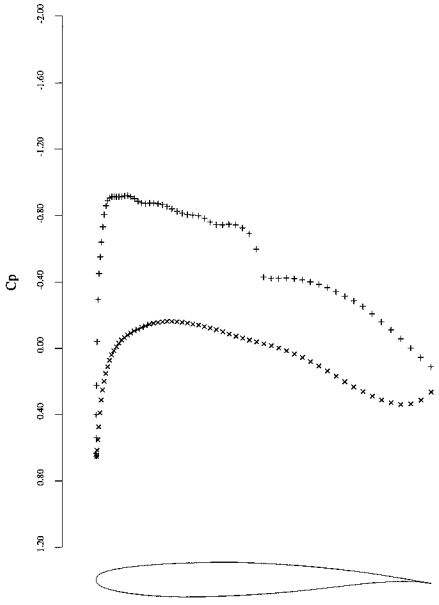

5c: span station $z = 0.625$

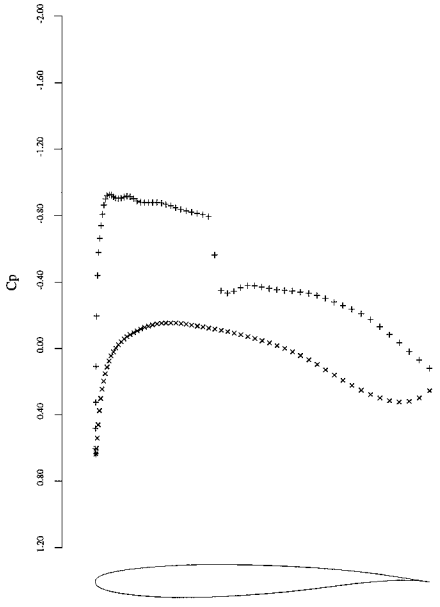

5d: span station $z = 0.937$

Figure 5: FLO67 check on redesigned wing.
$M = 0.85$, $C_L = 0.5051$, $C_D = 0.0099$, $\alpha = 0.0°$.

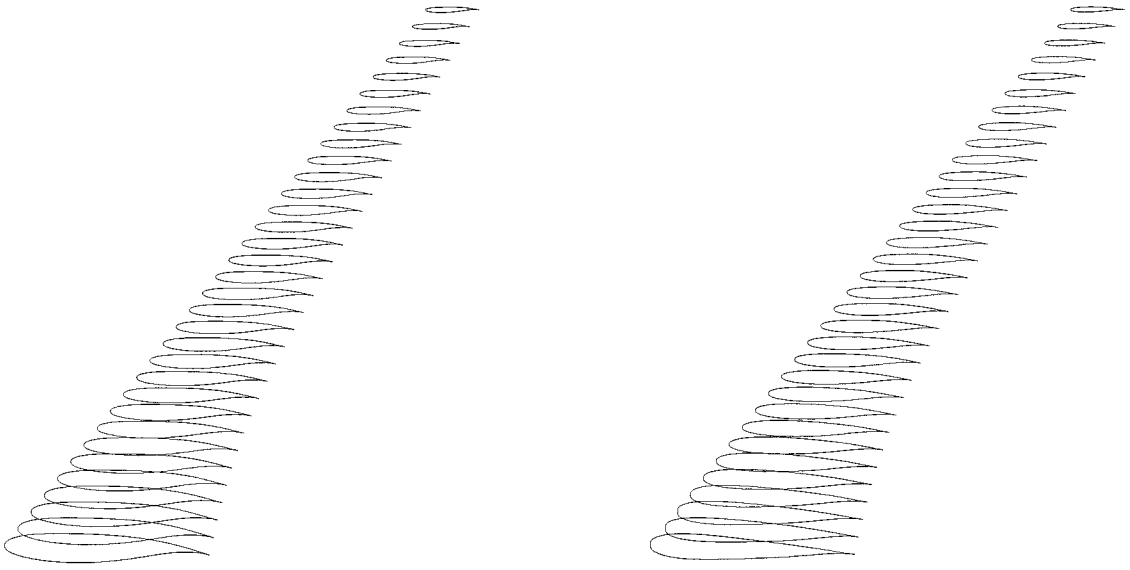

6a: Initial Wing
$C_l = 0.5500$, $C_d = 0.0243$, $\alpha = -0.962°$

6b: 10 Design Iterations
$C_l = 0.5500$, $C_d = 0.0144$, $\alpha = 0.274°$

Figure 6: Lifting Design Case, $M = 0.85$, Fixed Lift Mode.
Drag Reduction

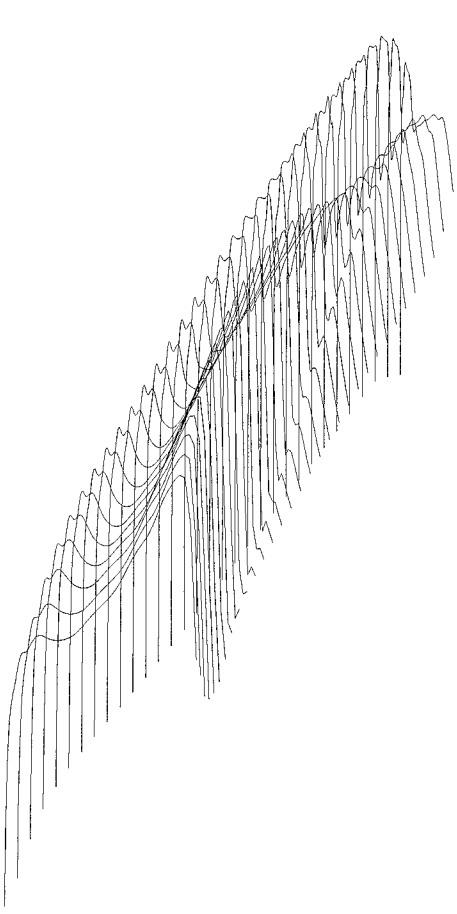

UPPER SURFACE PRESSURE

7a: Initial Wing
Lifting Design Case, $M = 0.85$, Fixed Lift Mode.
$C_L = 0.5500$, $C_D = 0.0243$, $\alpha = -0.962°$
Drag Reduction

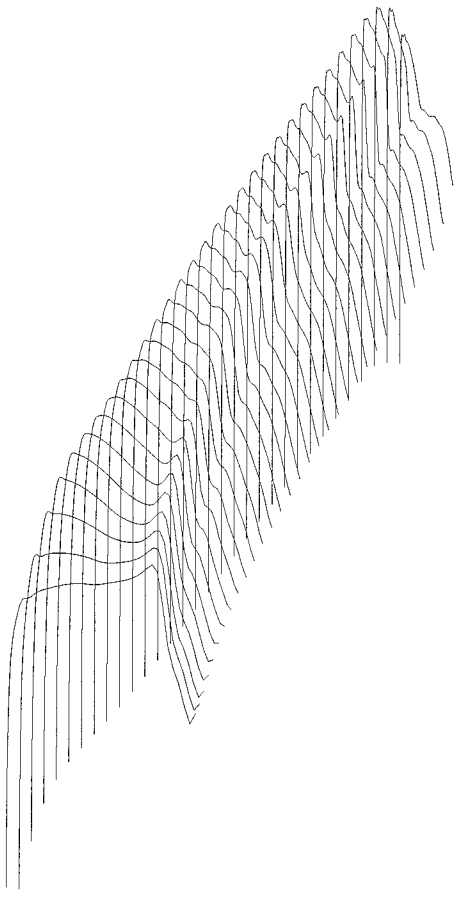

UPPER SURFACE PRESSURE

7b: 10 Design Iterations
Lifting Design Case, $M = 0.85$, Fixed Lift Mode.
$C_L = 0.5500$, $C_D = 0.0144$, $\alpha = 0.274°$
Drag Reduction

Figure 7: Lifting Design Case, $M = 0.85$, Fixed Lift Mode.
Drag Reduction

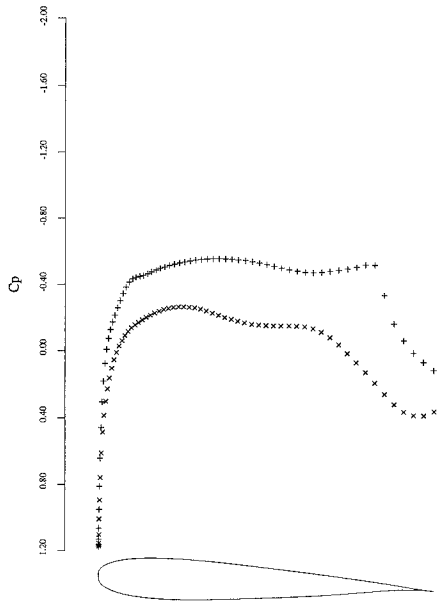

8a: span station $z = 0.00$

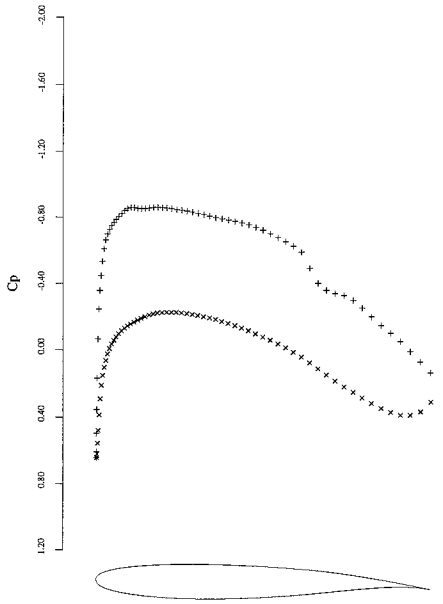

8b: span station $z = 0.312$

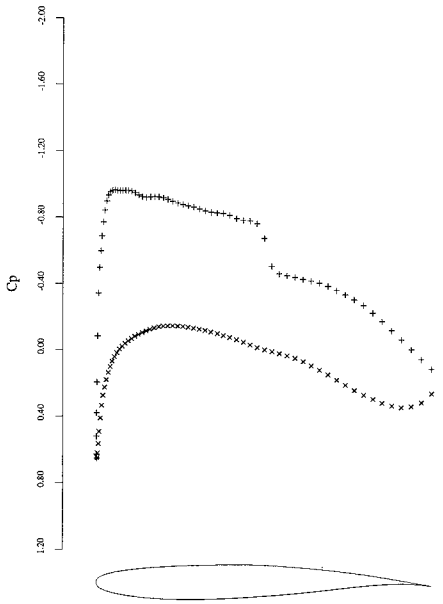

8c: span station $z = 0.625$

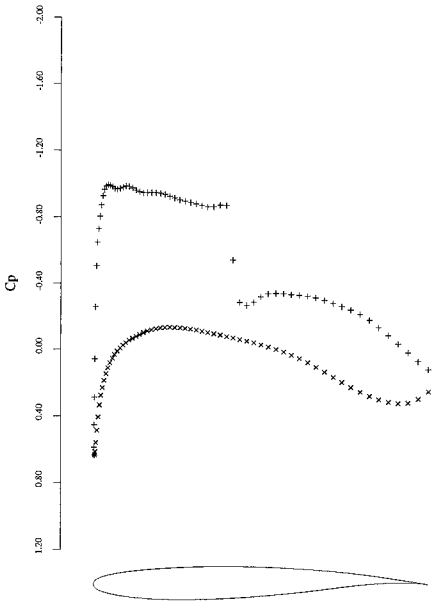

8d: span station $z = 0.937$

Figure 8: FLO67 check on redesigned wing.
$M = 0.85$, $C_L = 0.5500$, $C_D = 0.0119$, $\alpha = 0.210°$.